Selective Hydrogen Bonding Controls Temperature Response of Layer-by-Layer Upper Critical Solution Temperature Micellar Assemblies

Aliaksei Aliakseyeu,[1] Victoria Albright,[1] Danielle Yarbrough,[1] Samantha Hernandez,[2] Qing Zhou,[1] John F. Ankner,[3] and Svetlana A. Sukhishvili[1*]

[1]Department of Materials Science & Engineering, Texas A&M University, TX, 77843, USA

[2]College of Veterinary Medicine, Texas A&M University, TX, 77843, USA

[3]Spallation Neutron Source, Oak Ridge National Laboratory, 37831, TN, USA

Abstract

This work establishes a correlation between the selectivity of hydrogen-bonding interactions and the functionality of micelle-containing layer-by-layer (LbL) assemblies. Specifically, we explore LbL films formed by assembly of poly(methacrylic acid) (PMAA) and upper critical solution temperature block copolymer micelles (UCSTMs) composed of poly(acrylamide-*co*-acrylonitrile) P(AAm-*co*-AN) cores and polyvinylpyrrolidone (PVP) coronae. UCSTMs had a hydrated diameter of ~ 380 nm with a transition temperature between 45 and 50 °C, regardless of solution pH. Importantly, micelles were able to hydrogen-bond with PMAA, with the critical interaction pH being temperature dependent. To better understand the thermodynamic nature of these interactions, in depth studies using isothermal titration calorimetry (ITC) were conducted. ITC reveals opposite signs of enthalpies for binding of PMAA with micellar coronae vs. with the cores. Moreover, ITC indicates that pH directs the interactions of PMAA with micelles, selectively enabling binding with the micellar corona at pH 4 or with both the corona and the core at pH 3. We then explore UCSTM/PMAA LbL assemblies and show that the two distinct modes of PMAA

interaction with the micelles (*i.e.* whether or not PMAA binds with the core) had significant effects on the film composition, structure, and functionality. Consistent with PMAA hydrogen bonding with the P(AAm-*co*-AN) micellar cores, a significantly higher fraction of PMAA was found within the films assembled at pH 3 compared to pH 4 by both spectroscopic ellipsometry and neutron reflectometry. Selective interaction of PMAA with PVP coronae of the assembled micelles, achieved by the emergence of partial ionization of PMAA at pH 4 was critical for preserving film functionality demonstrated as temperature-controlled swelling and release of a model small molecule, pyrene. The work done here can be applied to a multitude of assembled polymer systems in order toto predict suppression/retention of their stimuli-responsive behavior.

Introduction

Multivalent intermolecular interactions lie at the heart of recognition and signal processes in biological and synthetic systems.[1,2] For example, multiple hydrogen bonds maintain the structure of biological molecules (proteins and DNA) and cause self-organization of synthetic block copolymers.[3,4] The collective nature of these interactions enables dramatic reorganization or dissociation of assembled structures in response to small changes in environmental stimuli.[5,6,7] One interesting class of synthetic stimuli-responsive material that exhibits such behavior is temperature-responsive polymers, which display temperature-switchable solubility in water.[8] The most studied responsive polymers are those with lower critical transition temperature (LCST) behavior,[9,10] such as PNIPAM, that demonstrate enhanced solubility upon a decrease in temperature. Upper critical solution temperature (UCST) polymer systems, that demonstrate enhanced solubility and/or swelling in response to an increase of environmental temperature, are

a relatively new development and are of significant interest for controlled delivery applications.[7,11,12] Such systems are controlled by polymer-polymer hydrogen bonding and have several advantageous properties, such as low sensitivity to ambient salt and facile tunability of the transition temperature.[13] UCST polymers can be synthesized as block copolymers so that one block microphase-separates at lower temperatures forming a core, due to extensive hydrogen-bonding between polymer units, while the other block remains water-soluble at all temperatures, thus forming a micellar corona. When exposed to higher temperatures, the core block becomes fully hydrated as the hydrogen bonds dissociate.[11,14]

Temperature responsiveness of micellar cores can be exploited to engineer adaptive surface coatings. Challenges can arise, however, in maintaining micellar functionality when they are attached to surfaces. For example, application of a stimulus can cause disassembly in monolayers of adsorbed micelles.[15] Co-assembly of polymer micelles with a binding partner within layer-by-layer (LbL) films can suppress such micellar disassembly. For example, in the case of polymer micelles with LCST cores, binding between micelles and a partner molecule (a linear synthetic polymer or a branched natural molecule, such as tannic acid) ensured the integrity of micelles within the films, which supported repeatable swelling transitions and temperature-controlled release of small molecules from surfaces.[16-19] Recently, our group has developed a family of UCSTMs and reported their incorporation within hydrogen-bonded LbL films. We showed that UCSTMs can be deposited on flat[11,14] or 3D substrates,[20] while retaining functionality in terms of temperature-triggered swelling and small molecule release.[12]

Yet retention of functionality of micellar LbL assemblies cannot yet be predicted, and failures to preserve micellar responsiveness are common. In the case of electrostatically assembled films of polymer micelles, a loss of film swelling response to temperature was attributed to

excessively strong binding between the micellar coronae and a LbL partner.[21] In hydrogen-bonded LbL films, crumpled micellar morphologies and inferior response to a temperature trigger occurred in assemblies stabilized exclusively by hydrogen bonding.[14] Interestingly, when a small amount of charge was applied to the partner molecule (tannic acid) via pH, LbL film response drastically improved. Here, we further explore correlations between modes of micelle/partner molecule binding and film response, focusing on a synthetic linear polymer rather than tannic acid as a binding partner, and explore the role of selective binding of the polymer partner with micellar corona *vs.* micellar core in retaining functionality of hydrogen-bonded micellar films.

Our specific system includes UCSTMs whose core- and corona-forming polymer blocks are composed of neutral polybases capable of hydrogen-bonding with a linear partner molecule – poly(carboxylic acid). We show that the pH-sensitive nature of hydrogen-bonding enables switching from binding of the polyacid with both polymer micellar blocks to exclusive binding with the micellar corona. To detect such switching, we employ isothermal titration calorimetry, ITC – a technique that yields the overall enthalpy and stoichiometry of intermolecular binding – to explore interactions of the polyacid and UCSTMs in solution. The ITC technique was earlier applied to explore thermodynamics of micellization and polymer complexes, study interactions between linear homopolymers used for LbL assembly, and correlate the enthalpy of formation of interpolymer complexes with the film growth mode.[22,23] In contrast, here we use ITC to study interactions of a linear polymer with responsive micelles composed of block copolymers. We demonstrate pH-control of selectivity in these interactions, and explore correlations between these interactions and composition, internal structure of LbL films, as well as the film's ability to support temperature-controlled swelling and small molecule release.

Materials and Methods

Materials. Acrylamide (AAm) (>99%, electrophoresis grade), cyanomethyl methyl(4-pyridyl)carbamodithioate (CMPC, 98%), and *p*-toluenesulfonic acid (*p*-TsOH, ≥98.5%) were used as received. Acrylonitrile (AN, ≥99%), 1-vinyl-2-pyrrolidinone (VP, ≥99%), and dimethyl sulfoxide (DMSO, ≥99%) were purified by distillation under vacuum. 2,2′-Azobis(2-methylpropionitrile) (AIBN, 98%) was recrystallized from methanol and dried under high vacuum before use. Branched polyethylenimine (BPEI with the weight-average molecular weight (M_w) of 750,000 g/mol), poly(vinyl pyrrolidone) (PVP, with M_w 55,000 g/mol) and sodium phosphate monobasic dihydrate were purchased from Sigma-Aldrich (Allentown, PA). Poly(methacrylic acid) (PMAA or *h*PMAA) (M_w 163 kDa, PDI <1.20) was purchased from Polymer Standard Services. Fully deuterated PMAA-d5 (*d*PMAA) with M_w 180 kDa and $M_w/M_n < 1.1$, *d*PMAA, were purchased from Polymer Source, Inc. Poly(methacrylic acid) with molecular weight of 175 kDA used for UV-Vis measurements was purchased from Scientific Polymer Products. Hydrochloric acid, sodium hydroxide, pyrene, and sulfuric acid were obtained from Alfa Aesar (Tewksbury, MA). Ultrapure water from a Milli-Q system (Merck Millipore, Burlington, MA, USA) with a resistivity of 18.2 MΩ was used in all experiments. Boron-doped silicon (Si) wafers, and undoped Si wafers used for FTIR analysis of LbL films were received from UniversityWafer Inc. (Boston, MA). All other chemicals were purchased from Sigma-Aldrich and used without further purification.

Synthesis and Characterization of Block Copolymers. Poly(acrylamide-*co*-acrylonitrile)-*b*-poly(vinyl pyrrolidone) block copolymer, P(AAm-*co*-AN)-*b*-PVP, was synthesized using RAFT polymerization as reported earlier,[14] and characterized using proton nuclear magnetic resonance (^{1}H NMR) and gel permeation chromatography (GPC). ^{1}H NMR was recorded in Texas A&M

Chemistry NMR facility using a Avance NEO 400 spectrometer in d_6-dimethyl sulfoxide (d_6-DMSO, Sigma Aldrich, 99.5% of deuterium) as a solvent. GPC measurements were performed with an Agilent 1260 Infinitive instrument equipped with a Phenogel 5 μm column (300 × 4.6 mm) column which was calibrated using poly(ethylene oxide) standards. DMSO as an eluent at a flow rate of 0.1 ml/min and a temperature of 45 ˚C were used. According to ^{1}H NMR and GPC analysis shown in **Figs. S1-S2**, the block copolymer contained 530 units of AAm and 125 units of AN in the AAm-AN block and 130 units of VP in the PVP block.

UV-Vis spectroscopy. Turbidity measurements were performed to confirm the temperature-controlled micellization of P(AAm-*co*-AN)-*b*-PVP as well as to probe pH-dependent formation of hydrogen-bonded complexes of P(AAm-*co*-AN)-*b*-PVP or control corona PVP blocks with PMAA. Turbidity was measured at a wavelength 700 nm using a Shimadzu UV 2600 spectrophotometer using temperature control of the cuvettes provided by a Julabo CORIO CD heating immersion circulator.

For studies of temperature-dependent micellization, we used 1 mg/ml solutions of P(AAm-*co*-AN)-*b*-PVP in PBS (0.01 M phosphate buffer containing 0.15 M sodium chloride). Heating and cooling rates were 1 ˚C/min.

For studies of hydrogen-bonded complexes, pH-adjusted solutions of the block copolymer or corona-forming PVP (with same molar concentration of PVP units (total concentration of P(AAm-*co*-AN)-*b*-PVP and PVP were 0.5 and 0.12 mg/ml, respectively)) and PMAA (0.48 mg/ml) were used within a wide range of pH from 2 to 8. After preheating at 55 ˚C for 30 minutes, PMAA solution was mixed with solutions of the block copolymer or PVP in the UV-vis cuvettes to achieve an equimolar ratio. Immediately after mixing, the cuvettes were placed in the UV-Vis spectrometer

and measured at a controlled temperature of 55 ˚C after a 5-minute equilibration. All solutions were then cooled at room temperature for 2 hours and measured at 25 ˚C.

Dynamic Light Scattering (DLS). Temperature dependences of hydrodynamic radius were measured with 2 mg/ml P(AAm-*co*-AN)-*b*-PVP solutions in PBS using a custom-made instrument which was equipped with a 532-nm 20-mW Whisper Mini Laser with a 0.5 mm beam diameter at a 90˚ scattering angle and a Luma 40 temperature-controlled cuvette holder (Quantum Northwest). Photon counts were detected using a fiber-optic adapter for the 8-mm photomultiplier tube model (Edmund Optics) and two Hamamatsu photon counters (H10682-210). The data was recorded and analyzed with the Corcle_v.0.18 software.

Transmission electron microscopy. UCSTMs were examined using a JEOL JEM-2010 transmission electron microscope (TEM) operating at 100 kV. The samples for TEM were prepared by drop-casting of 1 mg/ml micelles solutions on a carbon-coated copper grid (CF400-Cu-UL 400 mesh) supported by a filter paper. To minimize the effect of drying on micellar assembly, the samples were allowed to slowly dry at room temperature prior to analysis.

Isothermal Titration Calorimetry (ITC). For ITC, 0.165 mg/ml P(AAm-*co*-AN)-*b*-PVP solutions (1.5 mM of repeating units of AAm and 0.37 mM repeating units of VP), 0.11 mg/ml solutions of PVP (1 mM of repeat units of VP) in PBS and 1.56 mg/ml solution of PMAA (14.4 mM repeat units) in 0.01 M phosphate buffer. Because of the low sensitivity of hydrogen-bonded polymer assemblies to the presence of small ions,[24] the effects of buffer ions were expected to be minimal. pH-adjusted solutions were prepared the day before the experiment and equilibrated overnight. Prior to starting the experiment, pH was adjusted to pH 3 and 4 if needed. ITC measurements were performed using MicroCal VP-ITC (Malvern Instruments, Inc.) equipped with a 1.3959-ml cell at 25 ˚C and 55 ˚C. As a control experiment, PMAA solution was added to PBS

to determine the heat of dilution at both 25 ˚C and 55 ˚C. Experiments were performed at a constant stirring rate of 310 rpm using twenty-five 10-µl injections with 120-second waiting intervals between injections. After each titration, the cell was first rinsed with 1M NaOH solution to remove adsorbed hydrogen-bonded complexes from the cell walls, and then repeatedly rinsed with deionized water and the 0.01 M phosphate buffer of pH 3 and 4. All titrations were repeated twice.

Fourier Transform Infrared (FTIR) Spectroscopy. Two types of FTIR experiments were performed: the first one to probe the degree of ionization of free PMAA, and the second one to analyze composition of UCSTMs/PMAA LbL films. These experiments were conducted with dry powders of PMAA using KBr pellets, or with LbL films deposited on IR-transparent Si wafers, respectively. In the first case, 0.2 mg/mL solution of PMAA in Milli-Q water were adjusted to pH 3, 4 or 5 and freeze dried. The resulting powder samples were ground with potassium bromide (KBr), pressed into a pellet and analyzed by FTIR. To quantify the ionization degree, the absorbance of the band corresponding to asymmetric $>COO^-$ stretching vibrations at 1540 cm^{-1} was compared with that of the carbonyl vibration of non-ionized >COOH group at 1720 cm^{-1}.

In the second case, UCSTMs/PMAA LbL films were deposited onto undoped silicon wafers to allow for transmission FTIR measurements. For control experiments, solutions of PMAA or UCSTMs were drop casted and dried onto undoped silicon wafers. All samples were analyzed with a Tensor II spectrophotometer (Bruker Optics GmbH, Germany). Deconvolution of the peaks was performed using Origin Lab 2017 program. All peaks were fitted using Gaussian function.

Deposition of Layer-by-Layer Films. LbL films of P(AAm-*co*-AN)-*b*-PVP micelles and PMAA were deposited on silicon substrates using the LbL dip deposition technique. Prior to film construction, surfaces were primed by depositing a BPEI/PMAA bilayer *via* sequential 15-min

immersion in a 0.2 mg/ml BPEI solution in 0.01 M phosphate buffer at pH 9 and a 5-min immersion in a 0.2 mg/mL solution of PMAA in 0.01 M phosphate buffer at pH 3 or 4. Micellar films were then constructed at room temperature *via* alternating 5-min adsorption of UCSTMs (0.5 mg/ml solutions in PBS) and PMAA (0.2 mg/mL solutions in Milli-Q water). For control experiments, film deposition was conducted in a similar way, but UCSTM solution were replaced with 0.5 mg/ml PVP solution in PBS. In all deposition solutions, including rinsing solutions, pH was adjusted to 3 or 4.

Atomic Force Microscopy. Morphology of the UCSTMs was probed using a Bruker-Dimension Icon AFM instrument. The specimens were prepared as a monolayer of UCSTM micelles, or as a 2-bilayer film $(UCSTMs/PMAA)_2$ deposited on a BPEI/PMAA-primed silicon wafer from pH 3 or 4 solutions at room temperature. Imaging was carried out using a silicon cantilever with a normal stiffness of K n = 7.4 N/m and a resonance frequency of ~150 kHz.

Spectroscopic Ellipsometry. Thicknesses and optical constants of films in dry states were characterized by a variable angle spectroscopic ellipsometer (VASE, M-2000 UV−visible−NIR (240−1700 nm) J. A. Woollam Co., Inc., Lincoln, NE, USA) at four angles of incidence: 45°, 55°, 65° and 75°. Swelling measurements were done on the same ellipsometer equipped with a temperature-controlled liquid cell. For data fitting, polymeric layers were treated as a Cauchy material as described in our prior publication.[25]

Neutron Reflectometry (NR). For NR studies, LbL films were deposited on BPEI/PMAA-primed Si substrates in the following sequence: $[(UCSTM/h\text{PMAA})_8(UCSTM/d\text{PMAA})]_2$ $(UCSTM/h\text{PMAA})_8]$ at pH 3 and 4. Neutron reflectivity measurements were performed at the Spallation Neutron Source Liquids Reflectometer (SNS-LR) at the Oak Ridge National Laboratory (ORNL). The reflectivity data were collected using a sequence of 3.4-Å-wide continuous

wavelength bands (selected from 2.63 Å < λ < 16.63 Å) and incident angles (ranging over 0.6° < θ < 2.34°). The momentum transfer, $Q = (4\pi \sin\theta/\lambda)$, was varied over a range of 0.008 $Å^{-1} < Q < 0.20$ $Å^{-1}$. Reflectivity curves were assembled by combining seven different absolutely normalized wavelength and angle data sets together, maintaining a constant footprint and relative instrumental resolution of $\delta Q/Q = 0.023$ by varying the incident-beam apertures.

Scattering densities within hydrogenated and deuterated stacks were averaged, with each block exhibiting its characteristic thickness, scattering density, and interlayer roughness. Those characteristic parameters were adjusted until the reflectivity curve was best fitted (minimize χ^2).

Pyrene Loading and Release Studies. For pyrene release studies, 8-bilayer LbL films were deposited on 1 x 1 cm^2 pre-cleaned Si wafers using UCSTM and PMAA solutions at pH 3 or 4. To allow pyrene to absorb within the film, samples were exposed to 1 mg/mL solutions of pyrene in ethanol for 1 h. Afterwards, samples were washed with 0.01M phosphate buffer adjusted to pH 3 or 4 and dried. Pyrene was then released by soaking samples in 10 mL of the 0.01M phosphate buffer (with pH adjusted to pH 3 or 4) for 24 hours at 25 ˚C or 50 ˚C. All spectra were collected using a Shimadzu Scientific Instruments RF-6000 fluorescence spectrometer. The fluorescence spectra soaked were collected at an excitation wavelength $_{ex}$ of 320 nm, and measured at the emission maximum of pyrene $\boldsymbol{\lambda}_{em}$ of 371 nm.[11] To follow kinetics of the cumulative release of pyrene from the films, 3 mL aliquots of the total 10 mL release solution were taken at specific time points, measured, and quickly put back in the release solution.

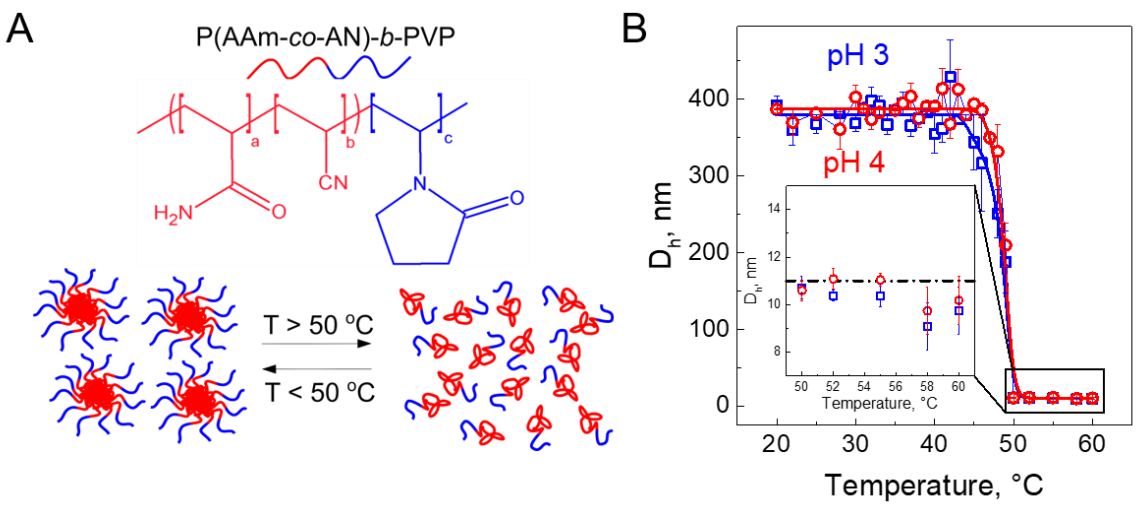

Figure 1. (A) Chemical structure of a UCST block copolymer and schematic representation of UCST-driven transition and (B) DLS measurements of hydrodynamic diameter (D_h) in 2 mg/ml P(AAm-*co*-AN)-*b*-PVP solutions in PBS as a function of temperature at pH 3 and 4. Inset represents D_h of the block copolymer above 50 °C.

Results and Discussion

Poly(acrylamide-*co*-acrylonitrile)-*b*-poly(vinyl pyrrolidone) (P(AAm-*co*-AN)-*b*-PVP) block copolymer was synthesized as reported in our earlier work.[14] The copolymer contained a temperature-responsive block composed of 530 units of AAm and 125 units of AN, and a hydrophilic PVP block composed of 130 units (**Fig. 1A**). The percentage of AAm units in the AAm-co-AN block (~20%) was chosen to ensure that the UCST transition occurred within the 45-50 °C temperature region. The strategy of varying the ratio between acrylamide to acrylonitrile units is a well-accepted tool for controlling UCST transitions.[26,27] **Fig. 1B** shows DLS measurements of hydrodynamic sizes of P(AAm-*co*-AN)-*b*-PVP block copolymer solutions as a function of temperature. At ambient temperature, UCSTMs formed consisting of P(AAm-*co*-AN) cores and PVP coronae having an average hydrodynamic diameter (D_h) of 384±17 nm with no significant difference between diameters at pH 3 and pH 4. The measured value of D_h is about

twice larger than two contour lengths of P(AAm-*co*-AN)-*b*-PVP chains, which are each composed of 785 units, indicating a high degree of water uptake by these UCSTMs. In the range of 45-50 ˚C, hydrodynamic diameters of the micellar assemblies sharply decreased (**Fig. 1B**), and above 50 ˚C (inset in **Fig. 1B**) only small diffusing species with the hydrodynamic diameters of 10±1 nm were present in solution. The size of these diffusing species is consistent with the size D_h of a random coil for the copolymer of 11.0 nm calculated from the characteristic ratio of 8.5 for PAAm in water[28] under assumption that R_g/R_h ratio of 1.26 for flexible chains in theta solvent.[29] Turbidity measurements (**Fig. S3)** confirm that the micelle-unimer transition temperature was not pH dependent, due to the absence of ionizable groups in the P(AAm-*co*-AN)-*b*-PVP chains. TEM imaging of the assembled structures (**Fig. S4**) confirmed micellar morphology with an average diameter of dry micelles of 200±55 nm as determined by analyzing images over 100 micelles. Similar to in solution data, micelles dried from solutions at pH 3 or 4 show no differences in average micelle diameter.

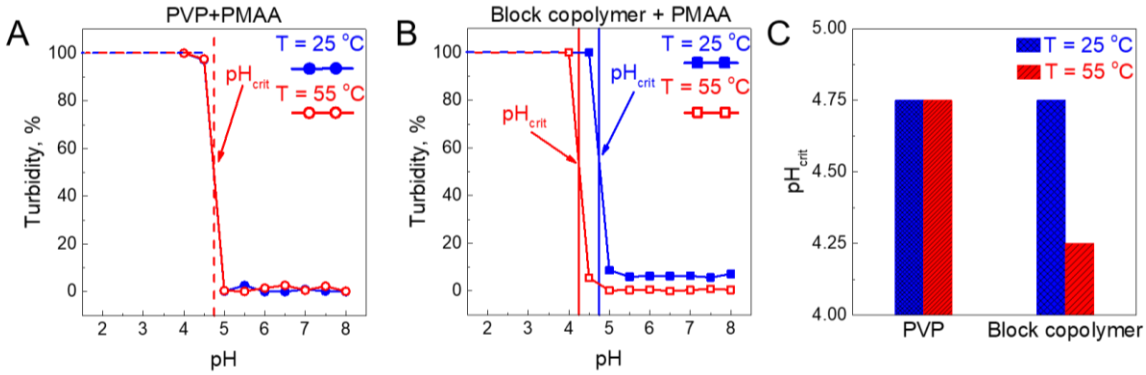

Figure 2. The effect of temperature on the turbidity of PVP/PMAA (A) and P(AAm-*co*-AN)-*b*-PVP/PMAA (B) solutions at 25 °C (closed symbols) and 55 °C (open symbols) measured at 700 nm, as well as a comparison of critical pH of IPC dissolution, pH_{crit}, for the two temperatures (C). All complexes were prepared at the equimolar concentration. pH_{crit} was determined as a pH at a half-height of turbidity in the transition region.

Next, we aimed to study the formation of hydrogen-bonded interpolymer complexes (IPCs) of PMAA with P(AAm-*co*-AN)-*b*-PVP or the corona-forming polymer (*i.e.* a PVP homopolymer) as a control. PMAA can hydrogen bond with both the corona-forming and core-forming micellar blocks resulting in stable complexes in acidic conditions. However, the effects of temperature and pH on binding of weak polycarboxylic acids with PVP and PAAm differ.[30-32,33] Previous studies have shown that at ambient temperatures, PAAm/PMAA complexes are less stable than PVP/PMAA complexes, with the critical pH_{crit} for IPC dissociation of 5 and 6.4, respectively.[24,34] In the case of PVP, alongside hydrogen bonding, hydrophobic interactions contribute to IPCs, which stabilizes IPCs at elevated temperatures.[5,30,35] In contrast, PAAm/PMAA interactions are primarily based on hydrogen bonding, and these complexes dissociate upon a temperature increase.[5,24] These trends are clearly seen in **Fig. 2**, which shows the effect of pH on the formation of PVP/PMAA and P(AAm-*co*-AN)-*b*-PVP/PMAA complexes at temperatures below and above UCST transition. The main result here is that as compared to PVP/PMAA complexes, pH_{crit} of P(AAm-*co*-AN)-*b*-PVP/PMAA IPCs is temperature-dependent. At 25 ˚C, pH_{crit} (4.75) remains the same for PVP/PMAA and UCSTMs/PMAA. Here, IPC formation is dominated by PVP/PMAA interactions, whether PVP chains are dissolved in solution or included in the micellar coronae. However, at an elevated temperature (55 ˚C) when the micelles are dissociated to individual block copolymer chains, pH_{crit} for dissociation of P(AAm-*co*-AN)-*b*-PVP/PMAA IPCs decreases to 4.25. The terminal pyridine groups (pK_a ~5.2[36]) remaining after RAFT polymerization are unlikely contributors to this process, because binding of individual pyridine groups with PMAA is much weaker than multisite polymer-polymer binding. Once the micelles dissociate, AAm-*co*-AN units become available for binding with PMAA and likely decrease the pH stability as PAAm/PMAA

complexes are less stable than PVP/PMAA complexes.[33] Turbidity results show a clear influence of temperature on IPC formation and IPC pH stability.

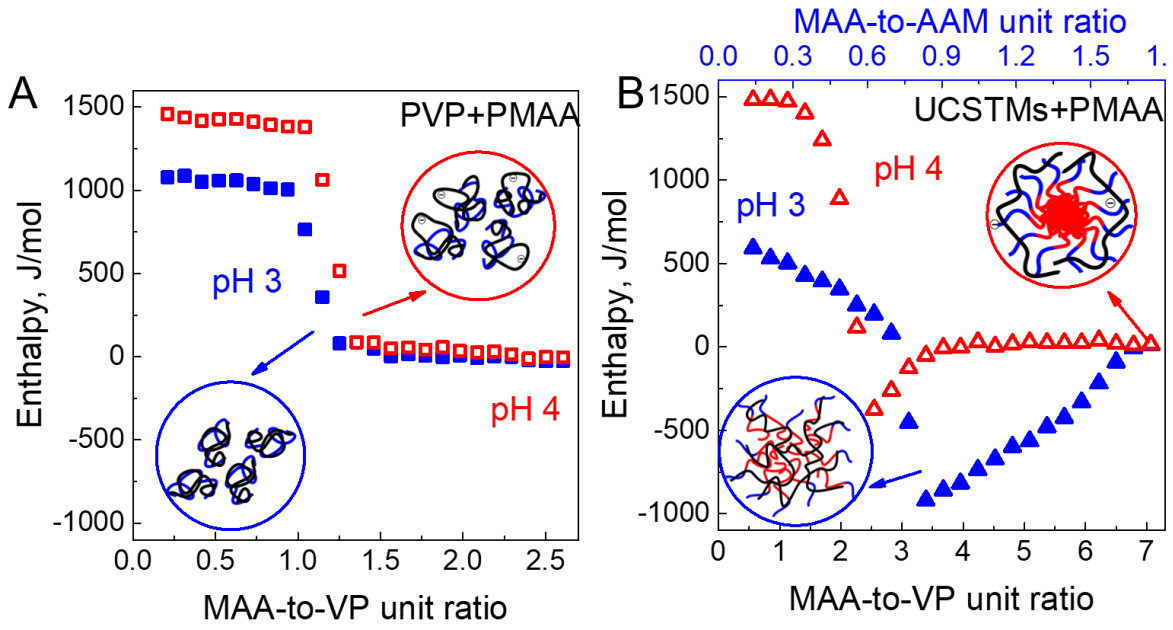

Figure 3. Isothermal titration calorimetry of PVP (squares) (A), and UCSTMs (triangles) (B) with PMAA at pH 3 (closed symbols) and pH 4 (open symbols) at 25 °C.

To further examine how pH influences the interactions of PMAA with P(AAm-*co*-AN)-*b*-PVP, we used the ITC technique. **Fig. 3** shows enthalpy changes during titration of PVP or UCSTMs with PMAA at 25 °C. In both systems, enthalpy (ΔH) of IPC formation was positive at the early stage of titration, suggesting a major role of hydrophobic interactions for binding of PMAA with PVP. For the titration of PVP homopolymer, ΔH determined per mole of PMAA repeating units was ~1.2 kJ/mol and ~1.5 kJ/mol at pH 3 and 4, respectively. These values were corrected by the enthalpy of dilution of PMAA in a polymer-free solution (**Fig. S5**), which was at least one order of magnitude lower than the enthalpy for polymer-polymer binding. The measured values of ΔH are higher than those previously reported for pH 2,[37] probably due to a lower concentration and different pH used in our experiments.

Fig. 3B shows the enthalpies for titration of UCSTM solutions (with PMAA), in which the concentration of PVP units was matched with that used in **Fig. 3A**. Here, there are two distinct regions with heat absorbed or released. At pH 3, in the beginning of the titration, PMAA/UCSTM binding is endothermic as PMAA interacts with PVP corona chains. The enthalpy switches its sign as the concentration of PMAA increases, and reaches its maximum negative value of –0.95 kJ/mol, which is very close to –1.0 kJ/mol previously reported for a PMAA/PAAm system.[37] These results reflect interaction of PMAA with both PVP and P(AAm-*co*-AN) blocks (*i.e.* penetration of PMAA within the micellar core) at pH 3, as illustrated in **Scheme 1A**. An increase of pH to 4 significantly altered PMAA/UCSTM interactions; the initial enthalpy (ΔH ~1.4 kJ/mol) was close to that observed for binding of PMAA with PVP homopolymer, and the region of the negative enthalpies related to PMAA/PAAm interactions was largely reduced at pH 4. This suggests the predominant binding of PMAA with the corona chains of the micelles at this pH. The drastically decreased interactions of the polyacid with the micellar cores correlate with emerging ionization of PMAA at pH 4 (pK_a of PMAA 6 - 7[38]) that created charge, which suppressed hydrogen-bonding. Ionization degrees of PMAA were directly determined here using FTIR analysis of PMAA samples, which were freeze-dried from solutions at pH 3 and 4 (**Fig. S6**), and gave values of 0% and 0.6% for pH 3 and 4, respectively. The 0.6% ionization of PMAA seems to be too low to suppress interpolymer binding, considering that a higher value of ~4% has been previously found for PAAM/PMAA homopolymers in their multilayer films.[24] The difference can be understood if one considers that here we used a copolymer of AAm rather than its homopolymer, as a micellar core block. The presence of acrylamide units in the copolymer disrupts the multisite hydrogen bonding between the core copolymer and PMAA, facilitating dissociation of PMAA/core complexes at a lower

critical pH and a lower ionization of the polyacid. **Scheme 1** summarizes the different modes of PMAA/micelle interactions in solutions of varied acidity.

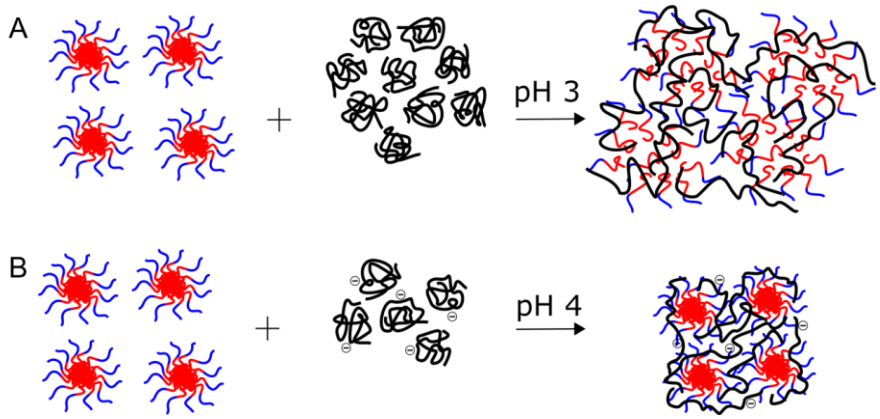

Scheme 1. Interactions of the polyacid with UCSTMs in solutions at pH 3 (A) and 4 (B) at 25 °C.

Whereas the data in **Fig. 3** were obtained at 25 °C, *i.e.* below the micellar UCST transition, **Fig. S7** shows the results from similar experiments performed at an increased temperature of 55 °C when polymer micelles were dissociated to individual block polymer chains. These results reveal trends similar to those seen in **Fig. 3**, with an even higher selectivity of binding of PMAA to micellar PVP corona at pH 4. The increased selectivity is probably due to the UCST behavior of P(AAm-*co*-AN)/PMAA complexes, which show weakening of intermolecular binding at increased temperatures[5] as shown at **Fig. 2**. Taken together, the results suggest that during micellar assembly with the polyacid in solution at pH 3, PMAA has penetrated the core of the micelles. However, slight ionization of PMAA at pH 4 suppresses binding of PMAA with the core polymer block, leading to increased selectivity of interactions.

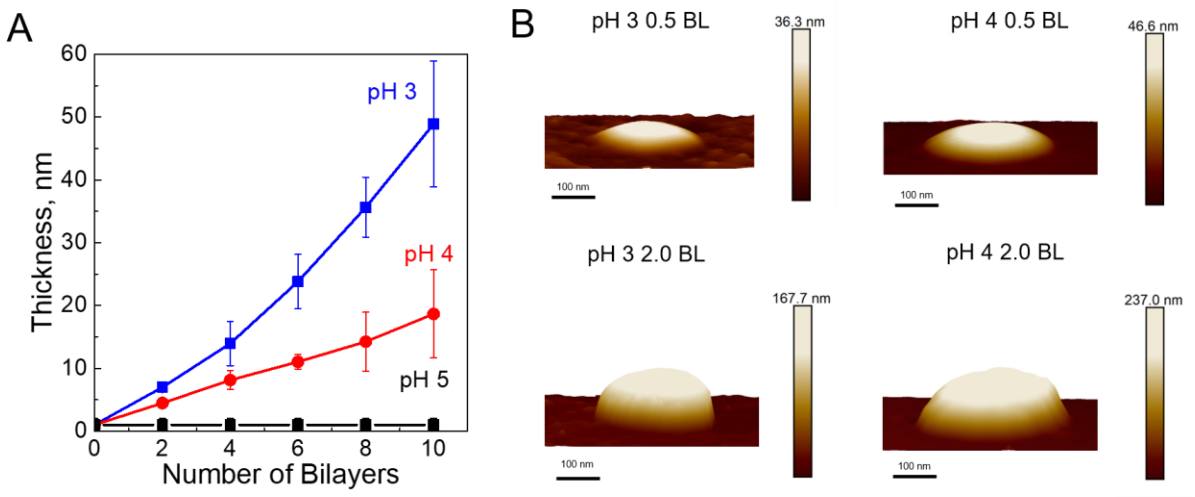

Figure 4. Dry thickness, as measured by spectroscopic ellipsometry of UCSTMs/PMAA films deposited at different pH at 25 °C (A). AFM topology images of a UCSTMs deposited within a monolayer or two-bilayer $(UCSTM/PMAA)_2$ coating deposited at pH 3 or 4 (B). All substrates were primed with BPEI/PMAA layer prior to deposition.

We then explored how pH-triggered control of the polyacid-micelle interactions affects functionality of the micelles when they are assembled within PMAA/UCSTM films. **Fig. 4A** illustrates pH-dependent growth of UCSTM/PMAA films deposited on silicon wafers covered with a BPEI/PMAA layer. FTIR spectra (**Fig. S8**) confirmed presence of both components in the film, determined from stretching >COOH vibrations of PMAA at 1710 cm^{-1} and amide I vibrations of the UCSTM core block at 1660 cm^{-1}, respectively. Ellipsometry data in **Fig. 4A** show that films deposited at pH 3, where PMAA was less ionized and intermolecular hydrogen-bonding was stronger, had 2.5-fold larger bilayer thickness than those built at pH 4 (5±1 nm vs. 2±0.5, respectively), and that film growth was completely inhibited at pH 5. For the control PVP/PMAA system, which exhibits critical pH of deposition in the same pH range (pH_{crit} 4.5),[24] the adsorbed amounts per bilayer thickness (**Fig. S9**) also decreased between pH 3 and 4.

To directly observe micellar morphology of LbL assemblies, UCSTMs were deposited within a monolayer or a two-bilayer $(UCSTM/PMAA)_2$ coating on a BPEI/PMAA-primed silicon wafer and studied with AFM. **Fig. 4B** shows that micelles deposited with an average radius and heights of 470± 240 nm and 42±12 nm at pH 3 and 580±110 nm and 40±5 nm at pH 4, respectively (**Fig. S10 A,B**). Therefore, within a monolayer, micelles had a high aspect ratio of 22±3, indicating that significant flattening of the micelles occurred as a result of drying, proximity to a solid surface, and interaction with the PMAA chains, as reported previously for other micellar systems.[18,39] In contrast, UCSTMs assembled further away from the substrate, *i.e.* within two-bilayer films, had a significantly lower aspect ratio of 1.9±0.2 as determined from their average radius and heights of ~120±90 nm and 160 ± 70 nm at pH 3 and 210 ± 70 nm and 220 ± 130 nm at pH 4, respectively (**Fig. S10 C, D**). In addition, the average micellar size was ~20-25% larger for micelles adsorbed at pH 4, probably because of charge-induced rigidification,[14] which in our case is caused by the emergence of charge on PMAA chains that are bound with the micellar corona.

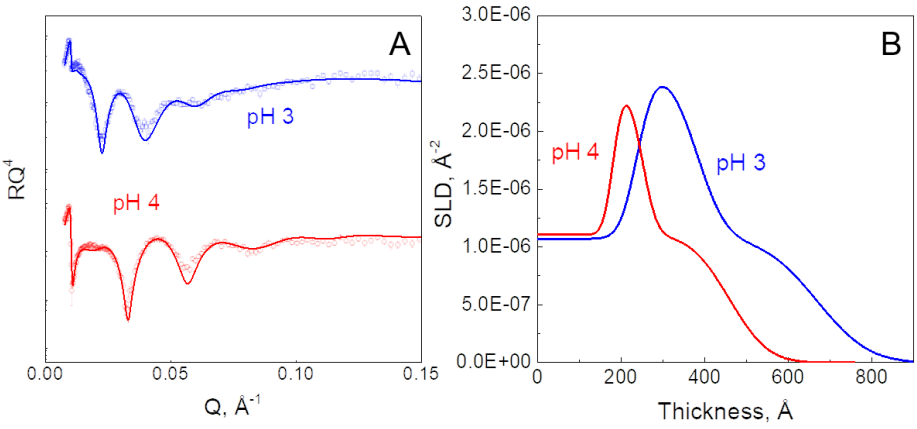

Figure 5. The effect of deposition solution pH on the internal structure of LbL films. Neutron reflectivity data (A - plotted as RQ^4 to enhance small features) and corresponding scattering length density profiles (B) for (UCSTM/*h*PMAA)$_8$/(UCSTM/*d*PMAA)$_2$/(UCSTM/*h*PMAA)$_8$ films deposited from solution with pH 3 and 4.

We then aimed to explore internal structure of PMAA/UCSTM films using neutron reflectometry (NR). To provide contrast for studies of the internal film structure, we used deuterated PMAA to construct LbL films with the following architecture: [(UCSTM/*h*PMAA)$_8$(UCSTM/*d*PMAA)]$_2$ (UCSTM/*h*PMAA)$_8$]. Data from NR studies can be seen in **Fig. 5.** For interpretation of NR results, we developed a fit model, described in detail in the SI, which includes parameters such as PMAA volume fraction per bilayer (f_{PMAA}) and bilayer thickness d_0. Fitting parameters and results of fitting can be seen in **Tables S1 and S2**.

In good agreement with the ellipsometry data, thickness per bilayer (d_0) for the film deposited at pH 3 was two-fold larger than that for the films constructed at pH 4 (44.7 Å vs. 24.2 Å, respectively). Also consistent with ellipsometry, films constructed at both pHs exhibited linear growth and were well-stratified, suggesting relatively low mobility of PMAA chains in the film during the time allowed for layer deposition. Importantly, the volume fraction of PMAA within the film determined from the NR fits was significantly different in the films deposited at pH 3 and

4 (0.82 ± 0.04 and 0.65 ± 0.04, respectively). This trend is consistent with the ITC data in **Fig. 3B**, which indicate that the weight fraction of PMAA consumed for binding with UCSTMs at pH 3 and 4 were 0.61 ± 0.04 and 0.45 ± 0.04, respectively. The larger amount of PMAA in the film was also confirmed using FTIR spectra. **Fig. S11** shows that the ratio of integrated intensities of stretching vibrations of PMAA to those of stretching vibrations of AAm units in the micellar core was 0.3±0.01 and 0.25±0.01 at pH 3 and 4, respectively. Taken together, the excess of PMAA in the pH 3 films confirmed by NR, FTIR, and ITC consistently show penetration of PMAA within UCSTM cores.

NR experiments have also revealed that the interfacial width at the *d*PMAA/*h*PMAA stack boundary is larger in the film deposited at pH 3 (~ 126 Å vs. ~ 63 Å at pH 4), which is probably related to higher amount of *d*PMAA deposited per bilayer. While in both cases stratification was preserved within the films, we hypothesize that films assembled at pH 4 will preferentially support temperature triggered responses because of the greater UCSTM content and preferential binding of PMAA with micellar coronae, which favors preservation of functionality of the micellar cores.

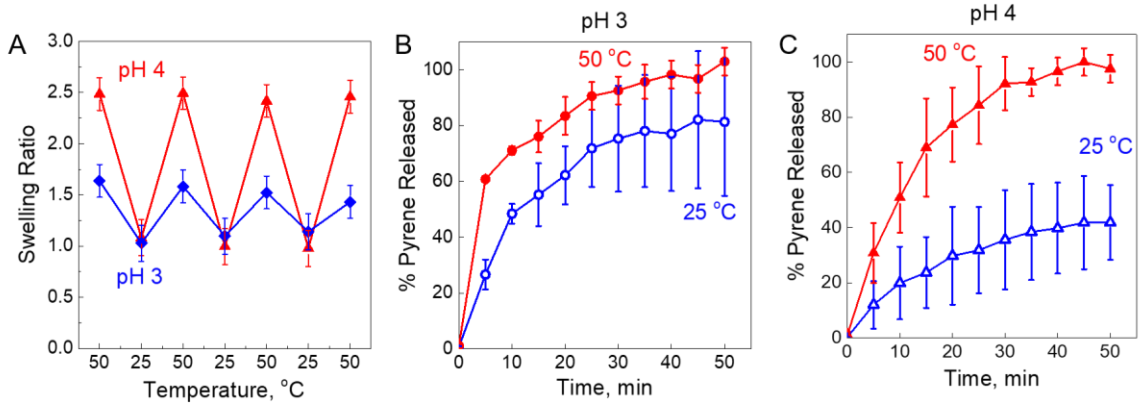

Figure 6. Swelling ratio of 8-bilayer UCSTM/PMAA films deposited at either pH 3 or 4 in 0.01 M phosphate buffer as measured by *in situ* spectroscopic ellipsometry. Temperature responsive release of pyrene as measured from 10 BL films deposited at pH 3 (B) or pH 4 (C).

To prove this hypothesis, we explored temperature-triggered swelling of UCSTM/PMAA films and their ability to control release of small molecules. **Fig. 6A** shows swelling response of micellar films subjected to repeated cycles of exposure to buffer solutions at 25 and 50 °C. Interestingly, significantly more water uptake occurred within the films deposited at pH 4, because of the predominant binding of PMAA with micellar corona rather than the cores and the overall weakened hydrogen-bonding interactions at pH 4. In contrast, P(AAm-*co*-AN) core units formed hydrogen bonds with PMAA at pH 3 and thus restricted film swelling.

We then explored the ability of these films to uptake and release a small model hydrophobic molecule – pyrene -- in response to temperature. Pyrene is robust fluorescent dye which is unable to participate in hydrogen bonding interactions with PMAA or PVP, but can be included within hydrophobic cores of the UCST micelles as shown previously.[11,40] Pyrene was loaded into the films and its release measured at temperatures below (25 ˚C) and above (50 ˚C) UCST as shown schematically in **Scheme 2**. While films were able to uptake and release pyrene (**Fig. 6 B and C**), only the films deposited at pH 4 demonstrated a robust temperature-controlled release of pyrene. At pH 3, PMAA interacted with both corona and core of the UCST micelles (**Fig. 3B**) retaining the ability to uptake pyrene, however, the release of pyrene was uncontrolled because the core/PMAA interactions inhibited the UCST response of the micellar cores. At the same time, selective binding of PMAA with corona of UCSTMs at pH 4 preserved the micellar cores, which enabled uptake and release of pyrene molecules in a temperature-controlled manner.

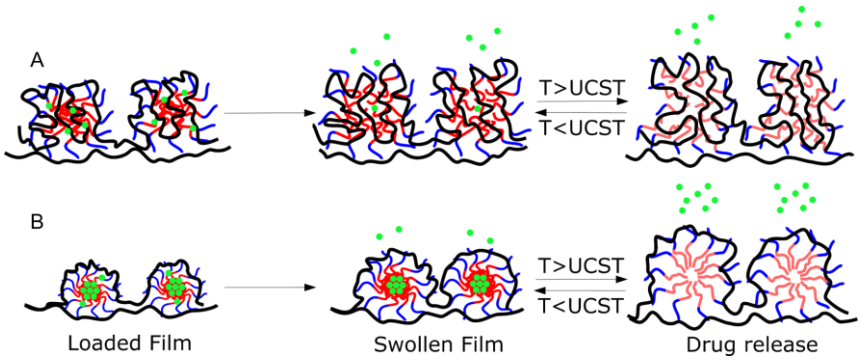

Scheme 2. Schematic representation of pyrene release at temperatures below (25 °C) and above (50 °C) UCST at pH 3 (A) and 4 (B).

Conclusion

In summary, we have shown that controlling the interactions of binding partners with block copolymer micelles can be crucial for maintaining temperature-responsive behavior of micellar LbL films. In noncovalent micellar assemblies, interactions of partner molecules with micellar cores can be tuned to suppress or preserve micellar temperature response. In hydrogen-bonded polymer systems, selectivity of interactions can be conveniently predicted by the ITC technique by taking advantage of the unique thermodynamics of aqueous UCST polymers as binding partners. While formation of most hydrogen-bonded complexes in aqueous solutions is driven entropically, UCST hydrogen-bonding polymers can exhibit enthalpically driven complex formation. When UCST polymers are included in micellar cores, penetration of the binding partner molecules with the micellar core leads to changes in the sign of binding enthalpy. Interactions of binding partner molecules with micellar cores has direct consequences on functionality of assembled LbL films, when polymer chains penetrate the core responsiveness of micellar films is suppressed. We show that by simply changing the deposition pH and thus ionization degree of a

weak polyacid, penetration of PMAA within the micellar core can be prevented and micellar film functionality can be preserved.

Acknowledgments

This work was supported by the National Science Foundation under Award DMR-1905535 (S.S.). A portion of this research used resources at the Spallation Neutron Source (Neutron Reflectometer, BL-4B), a DOE Office of Science User Facility operated by the Oak Ridge National Laboratory. Authors thank Anbazhagan Palanisamy for synthesis of the block copolymer used in the study, Dr. Mauricio Lasagna from the Department of Biochemistry and Biophysics of Texas A&M University for his help with ITC experiments and Raman Hlushko for helping with TEM imaging. The use of the TAMU Materials Characterization Facility and Microscopy and Imaging Center is acknowledged.

References

(1) Fasting, C.; Schalley, C. A.; Weber, M.; Seitz, O.; Hecht, S.; Koksch, B.; Dernedde, J.; Graf, C.; Knapp, E.-W.; Haag, R. Multivalency as a Chemical Organization and Action Principle. *Angewandte Chemie International Edition* **2012**, *51*, 10472-10498.

(2) Dubacheva, G. V.; Curk, T.; Mognetti, B. M.; Auzély-Velty, R.; Frenkel, D.; Richter, R. P. Superselective Targeting Using Multivalent Polymers. *Journal of the American Chemical Society* **2014**, *136*, 1722-1725.

(3) Altintas, O.; Artar, M.; ter Huurne, G.; Voets, I. K.; Palmans, A. R. A.; Barner-Kowollik, C.; Meijer, E. W. Design and Synthesis of Triblock Copolymers for Creating Complex Secondary Structures by Orthogonal Self-Assembly. *Macromolecules* **2015**, *48*, 8921-8932.

(4) Philp, D.; Stoddart, J. F. Self-Assembly in Natural and Unnatural Systems. *Angewandte Chemie International Edition in English* **1996**, *35*, 1154-1196.

(5) Zhuk, A.; Pavlukhina, S.; Sukhishvili, S. A. Hydrogen-Bonded Layer-by-Layer Temperature-Triggered Release Films. *Langmuir* **2009**, *25*, 14025-14029.

(6) Aoki, T.; Kawashima, M.; Katono, H.; Sanui, K.; Ogata, N.; Okano, T.; Sakurai, Y. Temperature-Responsive Interpenetrating Polymer Networks Constructed with Poly(acrylic acid) and Poly(N,N-dimethylacrylamide). *Macromolecules* **1994**, *27*, 947-952.

(7) Shimada, N.; Saito, M.; Shukuri, S.; Kuroyanagi, S.; Kuboki, T.; Kidoaki, S.; Nagai, T.; Maruyama, A. Reversible Monolayer/Spheroid Cell Culture Switching by UCST-Type Thermoresponsive Ureido Polymers. *ACS Applied Materials & Interfaces* **2016**, *8*, 31524-31529.

(8) Kotsuchibashi, Y.; Ebara, M.; Aoyagi, T.; Narain, R. Recent Advances in Dual Temperature Responsive Block Copolymers and Their Potential as Biomedical Applications. *Polymers* **2016**, *8*.

(9) Kim, Y.-J.; Matsunaga, Y. T. Thermo-responsive polymers and their application as smart biomaterials. *Journal of Materials Chemistry B* **2017**, *5*, 4307-4321.

(10) Zhou, Q.; Zhang, L.; Yang, T.; Wu, H. Stimuli-responsive polymeric micelles for drug delivery and cancer therapy. *International journal of nanomedicine* **2018**, *13*, 2921-2942.

(11) Palanisamy, A.; Albright, V.; Sukhishvili, S. A. Upper Critical Solution Temperature Layer-by-Layer Films of Polyamino acid-Based Micelles with Rapid, On-Demand Release Capability. *Chemistry of Materials* **2017**, *29*, 9084-9094.

(12) Albright, V.; Palanisamy, A.; Zhou, Q.; Selin, V.; Sukhishvili, S. A. Functional Surfaces through Controlled Assemblies of Upper Critical Solution Temperature Block and Star Copolymers. *Langmuir* **2019**, *35*, 10677-10688.

(13) Glatzel, S.; Laschewsky, A.; Lutz, J.-F. Well-Defined Uncharged Polymers with a Sharp UCST in Water and in Physiological Milieu. *Macromolecules* **2011**, *44*, 413-415.

(14) Palanisamy, A.; Sukhishvili, S. A. Swelling Transitions in Layer-by-Layer Assemblies of UCST Block Copolymer Micelles. *Macromolecules* **2018**, *51*, 3467-3476.

(15) Webber, G. B.; Wanless, E. J.; Armes, S. P.; Tang, Y.; Li, Y.; Biggs, S. Nano-Anemones: Stimulus-Responsive Copolymer-Micelle Surfaces. *Advanced Materials* **2004**, *16*, 1794-1798.

(16) Zhu, Z.; Gao, N.; Wang, H.; Sukhishvili, S. A. Temperature-triggered on-demand drug release enabled by hydrogen-bonded multilayers of block copolymer micelles. *Journal of Controlled Release* **2013**, *171*, 73-80.

(17) Zhu, Z.; Sukhishvili, S. A. Temperature-Induced Swelling and Small Molecule Release with Hydrogen-Bonded Multilayers of Block Copolymer Micelles. *ACS Nano* **2009**, *3*, 3595-3605.

(18) Xu, L.; Zhu, Z.; Sukhishvili, S. A. Polyelectrolyte Multilayers of Diblock Copolymer Micelles with Temperature-Responsive Cores. *Langmuir* **2011**, *27*, 409-415.

(19) Zhu, Z. C.; Sukhishvili, S. A. Layer-by-layer films of stimuli-responsive block copolymer micelles. *J Mater Chem* **2012**, *22*, 7667-7671.

(20) Albright, V.; Xu, M.; Palanisamy, A.; Cheng, J.; Stack, M.; Zhang, B.; Jayaraman, A.; Sukhishvili, S. A.; Wang, H. Micelle-Coated, Hierarchically Structured Nanofibers with Dual-Release Capability for Accelerated Wound Healing and Infection Control. *Advanced Healthcare Materials* **2018**, *7*, 1800132.

(21) Tan, W. S.; Cohen, R. E.; Rubner, M. F.; Sukhishvili, S. A. Temperature-Induced, Reversible Swelling Transitions in Multilayers of a Cationic Triblock Copolymer and a Polyacid. *Macromolecules* **2010**, *43*, 1950-1957.

(22) Loh, W.; Brinatti, C.; Tam, K. C. Use of isothermal titration calorimetry to study surfactant aggregation in colloidal systems. *Biochimica et Biophysica Acta (BBA) - General Subjects* **2016**, *1860*, 999-1016.

(23) Laugel, N.; Betscha, C.; Winterhalter, M.; Voegel, J.-C.; Schaaf, P.; Ball, V. Relationship between the Growth Regime of Polyelectrolyte Multilayers and the Polyanion/Polycation Complexation Enthalpy. *The Journal of Physical Chemistry B* **2006**, *110*, 19443-19449.

(24) Kharlampieva, E.; Sukhishvili, S. A. Hydrogen-Bonded Layer-by-Layer Polymer Films. *Journal of Macromolecular Science, Part C* **2006**, *46*, 377-395.

(25) Selin, V.; Albright, V.; Ankner, J. F.; Marin, A.; Andrianov, A. K.; Sukhishvili, S. A. Biocompatible Nanocoatings of Fluorinated Polyphosphazenes through Aqueous Assembly. *ACS Applied Materials & Interfaces* **2018**, *10*, 9756-9764.

(26) Asadujjaman, A.; Kent, B.; Bertin, A. Phase transition and aggregation behaviour of an UCST-type copolymer poly(acrylamide-co-acrylonitrile) in water: effect of acrylonitrile content, concentration in solution, copolymer chain length and presence of electrolyte. *Soft Matter* **2017**, *13*, 658-669.

(27) Huang, G.; Li, H.; Feng, S.-T.; Li, X.; Tong, G.; Liu, J.; Quan, C.; Jiang, Q.; Zhang, C.; Li, Z. Self-assembled UCST-Type Micelles as Potential Drug Carriers for Cancer Therapeutics. **2015**, *216*, 1014-1023.

(28) Bohdanecký, M.; Petrus, V.; Sedláček, B. Estimation of the characteristic ratio of polyacrylamide in water and in a mixed theta-solvent. **1983**, *184*, 2061-2073.

(29) Schmidt, M.; Burchard, W. Translational diffusion and hydrodynamic radius of unperturbed flexible chains. *Macromolecules* **1981**, *14*, 210-211.

(30) Khutoryanskiy, V. V.; Nurkeeva, Z. S.; Mun, G. A.; Dubolazov, A. V. Effect of temperature on aggregation/dissociation behavior of interpolymer complexes stabilized by hydrogen bonds. *Journal of Applied Polymer Science* **2004**, *93*, 1946-1950.

(31) Khutoryanskiy, V. V.; Dubolazov, A. V.; Mun, G. A.: pH- and Ionic Strength Effects on Interpolymer Complexation via Hydrogen-Bonding. In *Hydrogen-Bonded Interpolymer Complexes*; World Scientific, 2009; pp 1-21.

(32) Fortier-McGill, B.; Toader, V.; Reven, L. Chain Dynamics of Water-Saturated Hydrogen-Bonded Polymer Complexes and Multilayers. *Macromolecules* **2011**, *44*, 2755-2765.

(33) Sudre, G.; Tran, Y.; Creton, C.; Hourdet, D. pH/Temperature control of interpolymer complexation between poly(acrylic acid) and weak polybases in aqueous solutions. *Polymer* **2012**, *53*, 379-385.

(34) Kharlampieva, E.; Kozlovskaya, V.; Sukhishvili, S. A. Layer-by-Layer Hydrogen-Bonded Polymer Films: From Fundamentals to Applications. *Advanced Materials* **2009**, *21*, 3053-3065.

(35) Bekturov, E. A.; Bimendina, L. A.: Interpolymer complexes. In *Speciality Polymers*; Springer Berlin Heidelberg: Berlin, Heidelberg, 1981; pp 99-147.

(36) Mech, P.; Bogunia, M.; Nowacki, A.; Makowski, M. Calculations of pKa Values of Selected Pyridinium and Its N-Oxide Ions in Water and Acetonitrile. *The Journal of Physical Chemistry A* **2020**, *124*, 538-551.

(37) Bizley, S. C.; Williams, A. C.; Khutoryanskiy, V. V. Thermodynamic and kinetic properties of interpolymer complexes assessed by isothermal titration calorimetry and surface plasmon resonance. *Soft Matter* **2014**, *10*, 8254-8260.

(38) Izumrudov, V. A.; Kharlampieva, E.; Sukhishvili, S. A. Multilayers of a Globular Protein and a Weak Polyacid: Role of Polyacid Ionization in Growth and Decomposition in Salt Solutions. *Biomacromolecules* **2005**, *6*, 1782-1788.

(39) Talingting, M. R.; Ma, Y.; Simmons, C.; Webber, S. E. Adsorption of Cationic Polymer Micelles on Polyelectrolyte-Modified Surfaces. *Langmuir* **2000**, *16*, 862-865.

(40) Albright, V.; Xu, M.; Palanisamy, A.; Cheng, J.; Stack, M.; Zhang, B.; Jayaraman, A.; Sukhishvili, S. A.; Wang, H. Micelle-Coated, Hierarchically Structured Nanofibers with Dual-Release Capability for Accelerated Wound Healing and Infection Control. *Adv Healthc Mater* **2018**, *7*, e1800132.